iScience

CellPress
OPEN ACCESS

Article

Fat-body brummer lipase determines survival and cardiac function during starvation in *Drosophila melanogaster*

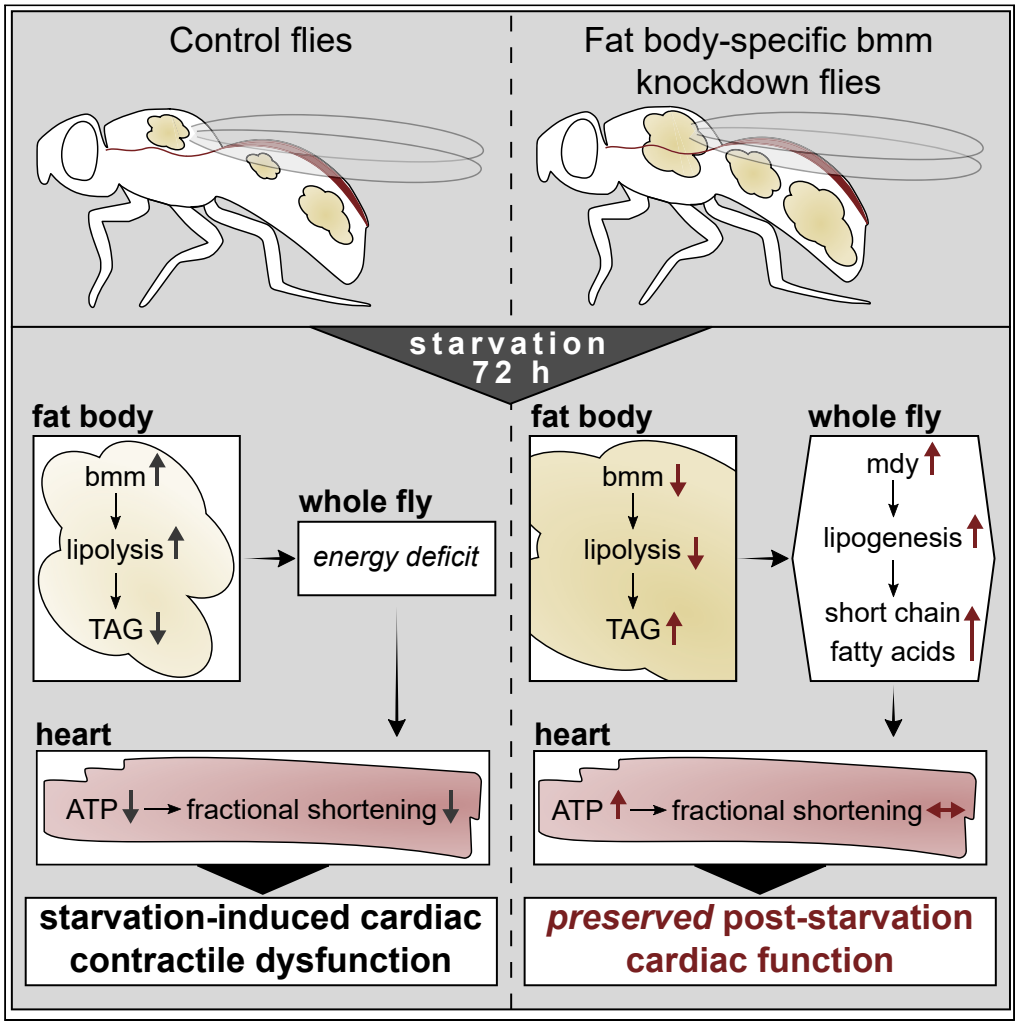

Annelie Blumrich, Georg Vogler, Sandra Dresen, ..., Stephan Sigrist, Rolf Bodmer, Ulrich Kintscher

ulrich.kintscher@charite.de

Highlights

A cross talk between fat body and the heart regulates cardiac function in *Drosophila*

Knockdown of fat-body brummer lipase prevents starvation-induced cardiac dysfunction

This involves preservation of lipid stores and maintenance of cardiac energy supply

Brummer-mediated preservation of fat body lipid stores involves lipolysis and lipogenesis

Blumrich et al., iScience *24*, 102288
April 23, 2021
https://doi.org/10.1016/j.isci.2021.102288

iScience

CellPress
OPEN ACCESS

Article

Fat-body brummer lipase determines survival and cardiac function during starvation in *Drosophila melanogaster*

Annelie Blumrich,[1,2,3] Georg Vogler,[3] Sandra Dresen,[1,2] Soda Balla Diop,[3] Carsten Jaeger,[4] Sarah Leberer,[1,2] Jana Grune,[2,5] Eva K. Wirth,[2,6] Beata Hoeft,[1,2] Kostja Renko,[7] Anna Foryst-Ludwig,[1,2] Joachim Spranger,[2,6] Stephan Sigrist,[8] Rolf Bodmer,[3,9] and Ulrich Kintscher[1,2,9,10,*]

SUMMARY

The cross talk between adipose tissue and the heart has an increasing importance for cardiac function under physiological and pathological conditions. This study characterizes the role of fat body lipolysis for cardiac function in *Drosophila melanogaster*. Perturbation of the function of the key lipolytic enzyme, *brummer* (*bmm*), an ortholog of the mammalian *ATGL* (adipose triglyceride lipase) exclusively in the fly's fat body, protected the heart against starvation-induced dysfunction. We further provide evidence that this protection is caused by the preservation of glycerolipid stores, resulting in a starvation-resistant maintenance of energy supply and adequate cardiac ATP synthesis. Finally, we suggest that alterations of lipolysis are tightly coupled to lipogenic processes, participating in the preservation of lipid energy substrates during starvation. Thus, we identified the inhibition of adipose tissue lipolysis and subsequent energy preservation as a protective mechanism against cardiac dysfunction during catabolic stress.

INTRODUCTION

Lipolysis is the enzymatic hydrolysis of triacylglycerol (TAG) to glycerol and fatty acids (FAs) (Zechner, 2015). The release of FAs from TAG storage provides a major energy source in situations of energy depletion or increased energy demand, and therefore, lipolysis represents a crucial determinant of energy homeostasis (Zechner, 2015). Adipose tissue is the central lipid storage organ with the highest lipolytic activity, thereby providing a large proportion of substrates for energy production in other organs (Ahmadian et al., 2011; Dube et al., 2015). Neutral lipolysis is catalyzed by different lipases among which adipose triglyceride lipase (ATGL) has been characterized as the key lipolytic enzyme in adipose tissue (Ahmadian et al., 2011; Haemmerle et al., 2006).

The heart is an organ that likely profits from adipose-derived energy supply, since it mainly relies on noncardiac energy substrates in order to generate adequate amounts of ATP for proper excitation and contraction (Bertero and Maack, 2018). This may become specifically significant under conditions characterized by energy deficits such as starvation. So far many interactions between adipose tissue and heart have been identified that can significantly affect cardiac function, but the focus of these studies was primarily on circulating mediators secreted from adipose tissue acting on the heart, such as the adipokines adiponectin, or leptin (Shibata et al., 2005; Sweeney, 2010). Much less is known, however, whether the adipose tissue energy storage controls cardiac energy metabolism and cardiac function by providing high-energy substrates, particularly during starvation.

The *Drosophila* ortholog of the mammalian ATGL is the gene *brummer* (*bmm* CG5295), the key lipolytic enzyme also in the fly's adipose tissue, the fat body (Gronke et al., 2005). Loss of *bmm* activity in flies resulted in progressively increased lipid storage and impaired TAG mobilization (Gronke et al., 2005). In this study we used *Drosophila melanogaster* as a model organism to investigate the relevance of lipolysis, in particular adipose tissue lipolysis, as an energy providing process, which determines cardiac function under energy-deprived conditions. We provide evidence that reducing lipolysis by knocking down *bmm* gene expression, specifically in *Drosophila* fat body, protects against starvation-induced cardiac dysfunction and significantly prolongs lifespan. Cardiac dysfunction was apparently caused by an exhaustion of high-energy

[1]Charité – Universitätsmedizin Berlin, Corporate Member of Freie Universität Berlin, Humboldt-Universität zu Berlin, and Berlin Institute of Health, Institute of Pharmacology, Center for Cardiovascular Research, CCR, Hessische Str. 3-4, 10115 Berlin, Germany

[2]DZHK (German Centre for Cardiovascular Research), Partner Site Berlin, Berlin, Germany

[3]Development, Aging and Regeneration Program, Sanford-Burnham-Prebys Medical Discovery Institute, La Jolla, CA 92037, USA

[4]Federal Institute for Materials Research and Testing (BAM), Berlin, Germany

[5]Charité – Universitätsmedizin Berlin, Corporate Member of Freie Universität Berlin, Humboldt-Universität zu Berlin, and Berlin Institute of Health, Institute of Physiology, Berlin, Germany

[6]Charité – Universitätsmedizin Berlin, Corporate Member of Freie Universität Berlin, Humboldt-Universität zu Berlin, and Berlin Institute of Health, Department of Endocrinology and Metabolism, Berlin, Germany

[7]Charité – Universitätsmedizin Berlin, Corporate Member of Freie Universität Berlin, Humboldt-Universität zu Berlin, and Berlin Institute of Health, Institute of Experimental Endocrinology, Berlin, Germany

[8]Institute of Biology/Genetics, Freie Universität Berlin, Berlin, Germany

[9]These authors contributed equally

[10]Lead contact

*Correspondence: ulrich.kintscher@charite.de

https://doi.org/10.1016/j.isci.2021.102288

substrates during starvation, whereas perturbation of fat body lipolysis led to enlarged TAG energy stores, higher levels of whole-body energy substrates and maintenance of myocardial energy supply. This is the first study showing that inhibition of *bmm*-mediated adipose lipolysis protects against cardiac dysfunction induced by energy depletion, a beneficial intervention that prolongs lifespan under these conditions. This protective action likely results from the preservation of adequate energy supply for proper cardiac function.

RESULTS

Bmm-mediated fat body lipolysis and heart function

To investigate the effects of fat body-specific lipolysis on heart function, *bmm* mRNA expression was reduced using the binary UAS-GAL4 system in combination with an RNA interference (RNAi) construct. To achieve a consistent and strong knockdown of *bmm* in the fat body, two different *bmm*-RNAi constructs were combined and expressed using the fat body-specific *ppl*-Gal4 driver (*ppl* > *bmm*RNAi^{2}). Fat body-specific *bmm* knockdown (*ppl* > *bmm*RNAi^{2} (fb*bmm*KD)) led to significantly diminished abdominal *bmm* mRNA levels in 2-week-old adult male flies compared with driver control flies (*ppl*/+) (Figure 1A). Consequently, whole-body TAG levels were significantly elevated in fb*bmm*KD flies (Figure 1B). This is in accordance with data from *bmm*mutant flies showing progressively increased lipid storage and impaired TAG mobilization (Gronke et al., 2005).

We next determined cardiac function in fb*bmm*KD and driver control flies under basal conditions in the fed state using the semi-automated optical heartbeat analysis (SOHA) (Figures S1A and S1B). fb*bmm*KD flies had normal cardiac function with respect to contractility, determined as fractional shortening, heart rate, or rhythmicity compared with controls (Figure S1B). There was a moderate but significant reduction in diastolic diameter in fb*bmm*KD flies (Figure S1B); however, this did not affect functional parameters like fractional shortening (Figure S1B). All in all, reduced *bmm*-mediated fat body lipolysis seems to have no major impact on cardiac function under basal conditions.

Starvation-induced cardiac dysfunction is rescued in fb*bmm*KD flies

To understand the relevance of adipose tissue lipolysis as an energy-providing process for adequate cardiac function, we next asked whether impaired lipolysis and TAG mobilization due to reduced *bmm*-mediated fat body lipolysis would affect cardiac function during times of energy deprivation. For this, flies were starved and both starvation resistance and cardiac function were analyzed. Stimulation of lipolysis under these conditions was indirectly documented by a marked increase of *bmm* mRNA expression in control flies under starvation (Figure 1C). This starvation-induced up-regulation was significantly attenuated in fb*bmm*KD flies (Figure 1C).

Of importance, fb*bmm*KD flies had significantly prolonged starvation survival compared with both driver and RNAi control flies (*ppl*/+ and *bmm*RNAi/+) (Figure 1D). Next, flies were starved or received normal food for 72 h followed by analysis of cardiac function using SOHA. In accordance with the starvation-mediated decrease of survival in control flies (*ppl*/+ and *bmm*RNAi/+), starvation of these flies caused a pronounced deterioration of cardiac function characterized by a marked reduction of contractility (fractional shortening) (Figures 1E and 1F). This alteration is indicative of primarily systolic dysfunction, i.e., an insufficiency in contractile ability, and was accompanied by enlarged systolic and, to a lesser degree, diastolic cardiac diameters (Figures 1E and 1F). Noteworthy, starvation-induced cardiac dysfunction was rescued in fb*bmm*KD flies including a preservation of fractional shortening and maintenance of normal systolic dimensions relative to ad-lib fed flies (Figures 1E and 1F).

Lack of fat body *bmm* preserves cardiac ATP-linked respiration

Cardiac dysfunction under catabolic stress may result from structural damage, a process called cardiac wasting (Springer et al., 2014). To understand whether starvation-induced cardiac structural defects are responsible for cardiac dysfunction in our model, we investigated the circumferential myofibril structure in cardiac tubes. No irregularities or degradation of myofibril structures were observed using a phalloidin stain (Figure 2A), suggesting that starvation-induced impairment of cardiac contractility in controls was not caused by structural defects of the heart tube.

To further understand preserved cardiac function upon starvation in fb*bmm*KD flies, we next investigated cardiac energy metabolism in fed and starved flies (Figures 2B–2D). For this, we established a novel, reproducible technique to assess mitochondrial function in adult *Drosophila* hearts. In particular, oxygen consumption rate was quantified directly in fly hearts using the Seahorse XFe Analyzer. The heart tubes of

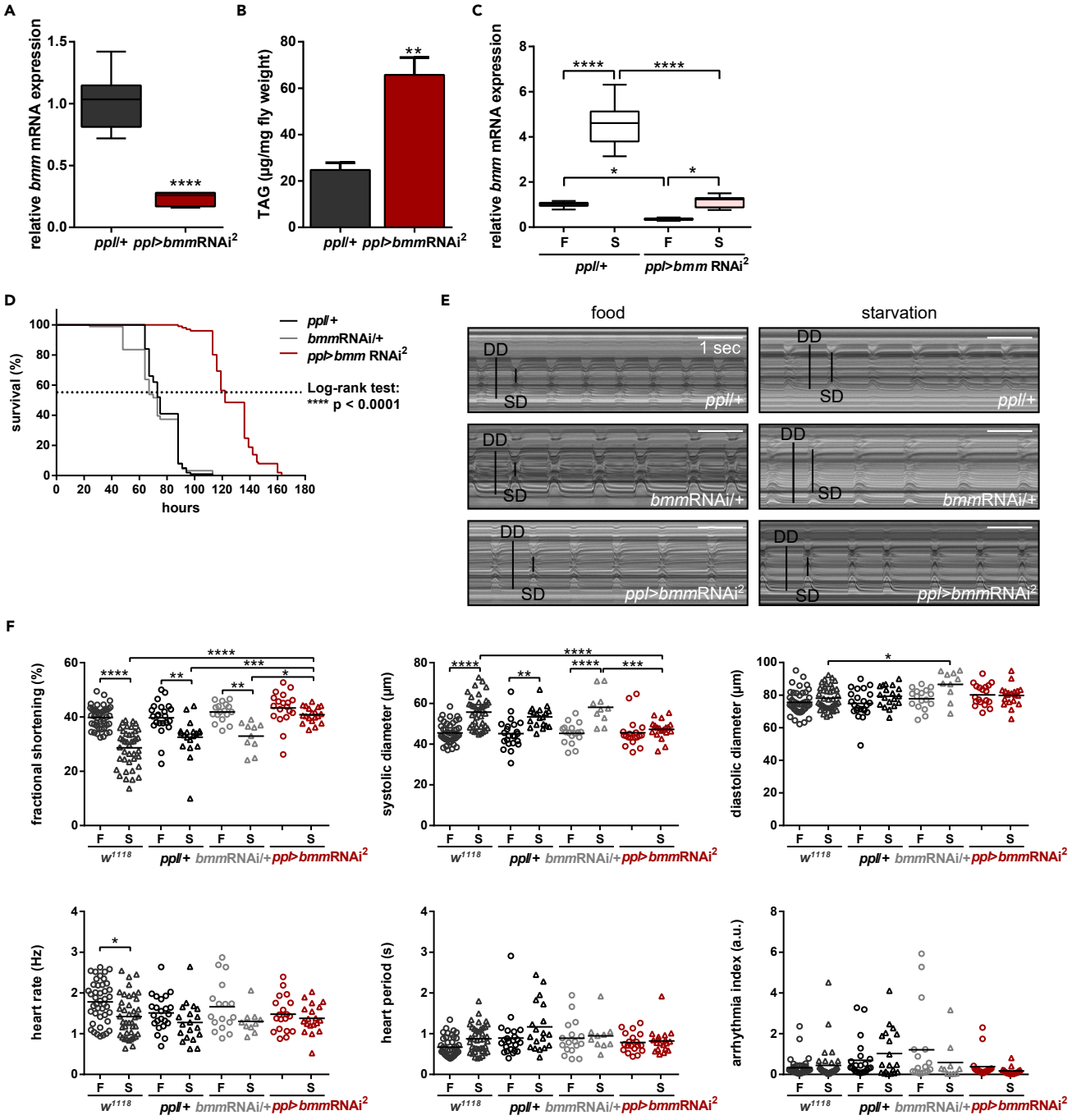

Figure 1. Starvation-induced cardiac dysfunction is rescued in fb*bmm*KD flies

(A) Relative *bmm* mRNA expression in abdomen of control (*ppl*/+) and fb*bmm*KD (*ppl* > *bmm*RNAi^2) flies under fed basal conditions (N = 3, n = 2–3 each 8–11 abdomen).

(B) Whole-body triacylglycerol level normalized to fly weight (N = 3, each n = 24 flies, mean +SEM).

(C) Relative *bmm* mRNA expression in whole flies under fed (F) and starved (S, 72 h) conditions (N = 3, n = 3 each 10 flies).

(D) Kaplan-Meier curve of starvation survival. About 90–110 flies per group were starved and survival was examined every 3 h during daytime.

(E) Representative M-modes from SOHA recordings from fed and starved (72 h) flies. DD, diastolic diameter; SD, systolic diameter.

(F) Heart function parameters determined using SOHA of fed (F) and starved (72 h) (S) flies (N = 3, n = 10–23, mean).

(A and B) Unpaired t test, **p < 0.01, ****p < 0.0001. (D) Log rank test, ****p < 0.0001. (C + F) Two-way ANOVA, Bonferroni post hoc test, arrhythmia index: Kruskal-Wallis test, Dunn's post hoc test; *p < 0.05, **p < 0.01, ***p < 0.001, ****p < 0.0001.

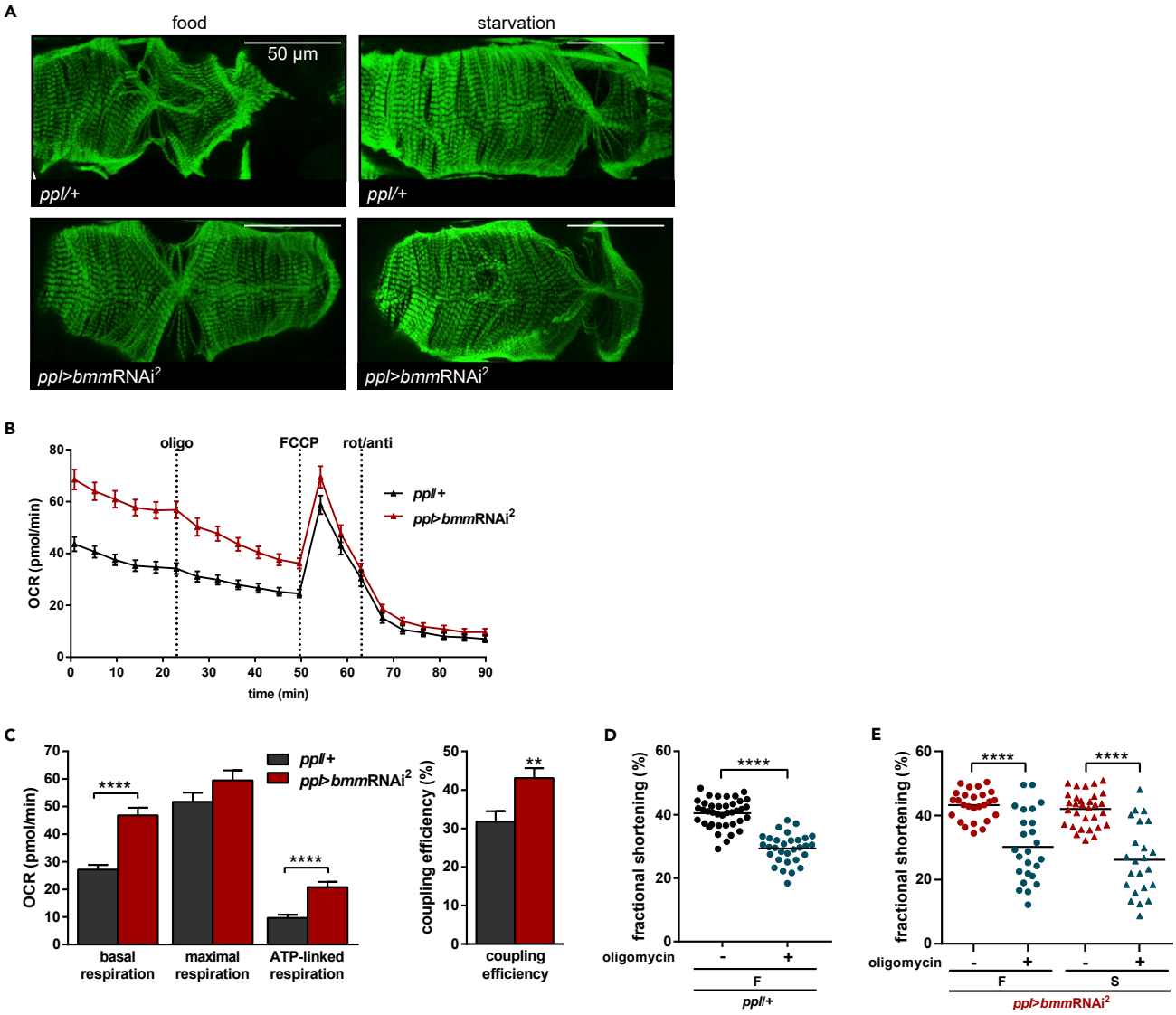

Figure 2. Lack of fat body *bmm* preserves cardiac ATP-linked respiration

(A) Representative pictures of stained F-actin (green) in cardiac tubes from control and fb*bmm*KD flies under fed and starved (72 h) conditions. Images were taken at the abdominal segment 2–3, where the third pair of ostial cells is located. Scale bar, 50 µm.

(B and C) (B) Analysis of the oxygen consumption rate and (C) quantification of basal, maximal, and ATP-linked respiration, and coupling efficiency (% of basal respiration used to drive ATP synthesis) from starved beating heart tubes of control (*ppl*/+) and fb*bmm*KD (*ppl* > *bmm*RNAi^{2}) flies. (N = 3, n = 36, mean +SEM, unpaired t test, **p < 0.01, ****p < 0.0001).

(D) Fractional shortening from SOHA analysis of (*ppl*/+)-control flies in the presence of oligomycin (2.5 µM, blue symbols) or vehicle control (DMSO) for 10 min prior to heart function analysis. (N = 3, n = 31–39, mean, two-way ANOVA, Bonferroni post hoc test, ****p < 0.0001).

(E) Fractional shortening from SOHA analysis of fb*bmm*KD (*ppl* > *bmm*RNAi^{2}) flies under fed and starved conditions in the presence of oligomycin (2.5 µM, blue symbols) or vehicle control (DMSO) for 10 min prior to heart function analysis. (N = 4, n = 23–31, mean, two-way ANOVA, Bonferroni post hoc test, ****p < 0.0001). OCR, oxygen consumption rate; oligo, oligomycin; FCCP, carbonyl cyanide-p-trifluoromethoxyphenylhydrazone; rot/anti, rotenone/antimycin (A).

starved fb*bmm*KD flies showed markedly higher rates of basal respiration and ATP-linked respiration accompanied by an improved coupling efficiency when compared with control flies (Figures 2B and 2C). Accordingly, when we blocked ATP-synthase by oligomycin in control flies and analyzed cardiac contractility, inhibition of ATP synthesis clearly mimicked the impairment of contractility observed under starvation (Figure 2D). Blockade of the ATP synthase by oligomycin also reduced contractility in fb*bmm*KD flies under fed and starved conditions (Figure 2E).

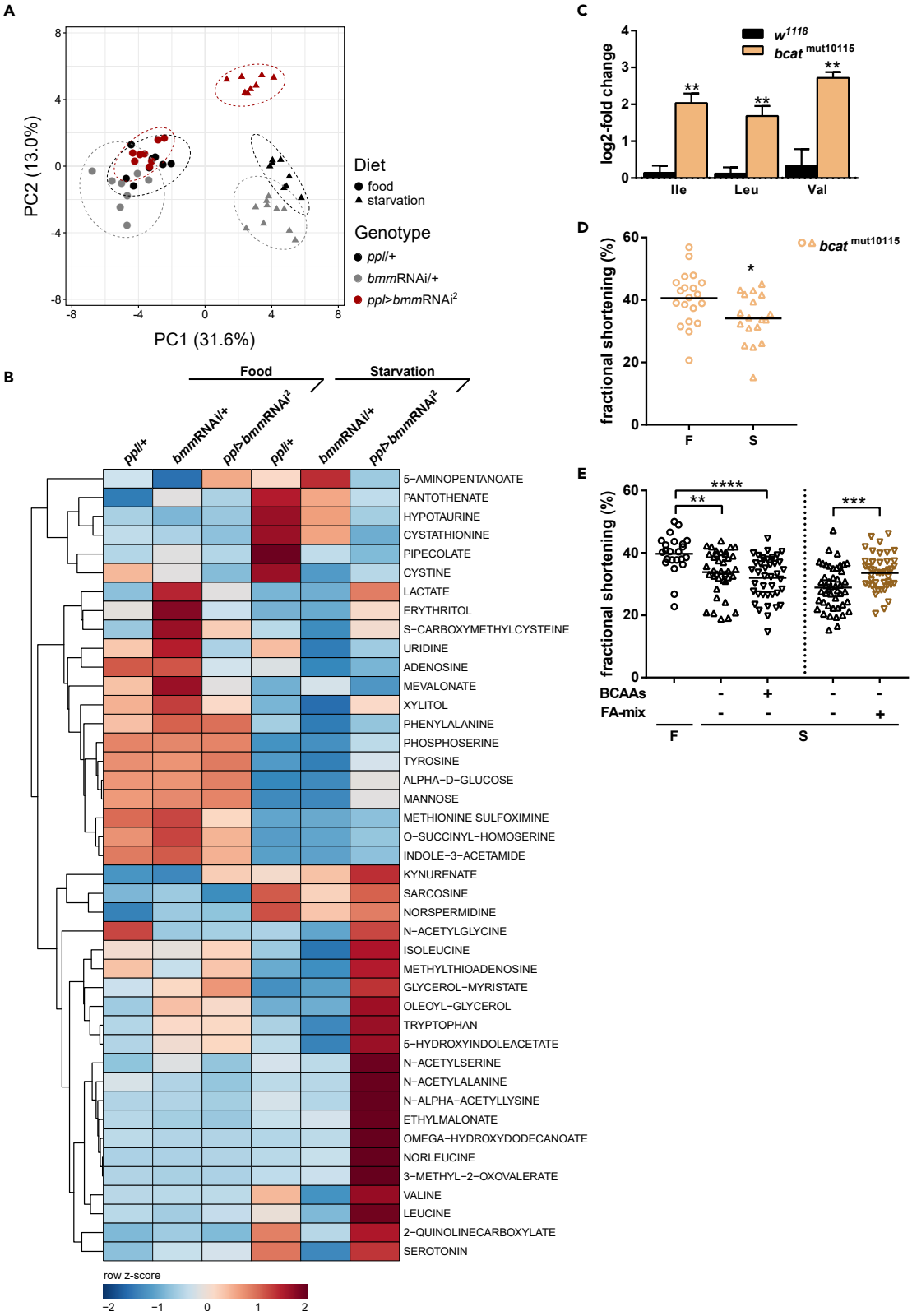
A
PC2 (13.0%)
PC1 (31.6%)
Diet
food
starvation
Genotype
ppl/+
bmmRNAi/+
ppl>bmmRNAi2
B
Food
Starvation
ppl/+
bmmRNAi/+
ppl>bmmRNAi2
ppl/+
bmmRNAi/+
ppl>bmmRNAi2
5−AMINOPENTANOATE
PANTOTHENATE
HYPOTAURINE
CYSTATHIONINE
PIPECOLATE
CYSTINE
LACTATE
ERYTHRITOL
S−CARBOXYMETHYLCYSTEINE
URIDINE
ADENOSINE
MEVALONATE
XYLITOL
PHENYLALANINE
PHOSPHOSERINE
TYROSINE
ALPHA−D−GLUCOSE
MANNOSE
METHIONINE SULFOXIMINE
O−SUCCINYL−HOMOSERINE
INDOLE−3−ACETAMIDE
KYNURENATE
SARCOSINE
NORSPERMIDINE
N−ACETYLGLYCINE
ISOLEUCINE
METHYLTHIOADENOSINE
GLYCEROL−MYRISTATE
OLEOYL−GLYCEROL
TRYPTOPHAN
5−HYDROXYINDOLEACETATE
N−ACETYLSERINE
N−ACETYLALANINE
N−ALPHA−ACETYLLYSINE
ETHYLMALONATE
OMEGA−HYDROXYDODECANOATE
NORLEUCINE
3−METHYL−2−OXOVALERATE
VALINE
LEUCINE
2−QUINOLINECARBOXYLATE
SEROTONIN
row z-score
C
w1118
bcat mut10115
log2-fold change
Ile
Leu
Val
D
bcat mut10115
fractional shortening (%)
F
S
E
fractional shortening (%)
BCAAs
FA-mix
F
S

Figure 3. Starved fb*bmm*KD flies have elevated whole-body energy substrates

(A and B) Analysis of control (*ppl*/+ and *bmm*RNAi/+) and fb*bmm*KD (*ppl* > *bmm*RNAi^{2}) flies under fed and starved (72 h) conditions. Polar metabolite profiling using GC-MS of whole flies. (A) Principal component analysis, dashed ellipses indicate 95% confidence interval. (B) Heatmap and hierarchical clustering of 42 metabolites that were significantly regulated (two-way ANOVA, diet-genotype interaction, adjusted $p < 0.05$).

(C) GC-MS-based analysis of 2-week-old male *bcat* ^{mut10115} and w^{1118} control flies. Isoleucine, leucine and valine were significantly elevated in *bcat* ^{mut10115} compared with w^{1118}. Unpaired t test, $^{**}p < 0.01$.

(D) Fractional shortening from SOHA analysis of *bcat* ^{mut10115}. Flies were starved for 37–41 h (S) or received normal food (F). (N = 2, n = 20/18, mean). Unpaired t test, $^{*}p < 0.05$.

(E) Fractional shortening from SOHA analysis of fed (F) and starved (72 h) (S) *ppl*/+ flies. Flies received branched-chain amino acids (BCAA) (BCAAs +: 10 mM Ile, 10 mM Leu, 10 mM Val) or H_2O (BCAAs) as control (F: N = 3, n = 23, S: N = 3, n = 38/41, mean). Furthermore, fractional shortening from SOHA analysis of starved *ppl*/+ flies receiving lipid-rich BSA in saline (FA-mix) was determined. (N = 3, n = 46/44, mean). One-way ANOVA, Bonferroni post hoc test, $^{**}p < 0.01$, $^{****}p < 0.0001$ (BCAA). Unpaired t test, $^{***}p < 0.001$ (FA-mix).

Together these data suggest that the preservation of cardiac function under starvation in fb*bmm*KD flies may have been caused by a starvation-resistant maintenance of adequate cardiac ATP synthesis. We next asked the question whether this improved cardiac ATP-linked respiration may have resulted from an enhanced systemic energy substrate supply under starvation. This would be consistent with observations in *bmm* mutant flies under starvation, which, due to their increased TAG stores, are able to maintain systemic metabolism for a prolonged period of time through sustained supply of energy substrates (Gronke et al., 2005).

Starved fb*bmm*KD flies have elevated whole-body energy substrates

To investigate the metabolic status and systemic energy metabolism in fed and starved flies, we first carried out metabolite profiling using mass spectrometry (Figures 3A and 3B). Principal component analysis was performed to simplify the dataset and visualize patterns (Figure 3A). The largest variance of the metabolite profile was caused by dietary intervention, i.e., food versus starvation (Figure 3A). In addition, starved fb*bmm*KD flies had a distinctly different metabolite profile compared with that of starved controls (Figure 3A). Hierarchical clustering of significantly regulated metabolites revealed a clear distinction between fed and starved flies independent of the genotype (Figure 3B). Of more importance, fb*bmm*KD flies carried significantly higher levels of metabolites involved in energy metabolism compared with starved control groups (Figure 3B). Of note, branched-chain amino acids (BCAAs) including isoleucine, leucine, and valine and distinct lipid intermediates such as glycerol myristate and oleoyl-glycerol were markedly higher in starved fb*bmm*KD flies, even than in fed fb*bmm*KD flies (Figure 3B). These data provide evidence that during starvation fb*bmm*KD flies are capable of maintaining higher systemic energy substrate/metabolite levels, a process likely involved in their preserved cardiac function and prolonged starvation survival.

To clarify whether increased systemic metabolite levels mediate cardioprotection in starved fb*bmm*KD flies, we first started to investigate the role of BCAAs. For this we utilized a *Drosophila* model with increased systemic BCAA levels. The branched-chain amino acid transferase (BCAT) mediates the initial step in BCAA catabolism and regulates BCAA levels (Neinast et al., 2019). Accordingly, $bcat^{mut10115}$ flies exhibit increased systemic BCAA levels (Figure 3C) similarly to starved fb*bmm*KD flies. When we challenged these flies with prolonged starvation, cardiac systolic function (fractional shortening) was still significantly impaired (Figures 3D and S2A), despite the high levels of BCAAs (Figure 3C). Likewise, addition of BCAAs did not improve fractional shortening of starved control flies (*ppl*/+) (Figures 3E and S2B, left). These data make it unlikely that BCAAs are involved in the protection against starvation-induced cardiac dysfunction, even in fb*bmm*KD flies.

Of interest, adding a fatty acid (FA) mixture containing distinct FAs (C16:0; C18:0, C18:1, C18:2, C18:3), instead of BCAAs, led to a significantly improved fractional shortening and partial rescue in starved *ppl*/+ flies (Figures 3E and S2B, right), compared with saline alone. Together with the increased levels of lipid intermediates (Figure 3B), such as glycerol-myristate or oleoyl-glycerol, these results point toward a possible role of lipids in fb*bmm*KD flies as the rescuing high-energy substrate for the starved myocardium.

fb*bmm*KD flies maintain high levels of glycerolipids and phosphatidylcholines under starvation

In order to gain more precise insights into the regulation and relevance of lipids in starved-fb*bmm*KD flies, we conducted an LC-MS-based lipidomics analysis in fed and starved flies. In the principal component analysis, a marked variance of the lipid profile was caused by diet in control flies, which was absent in fb*bmm*KD

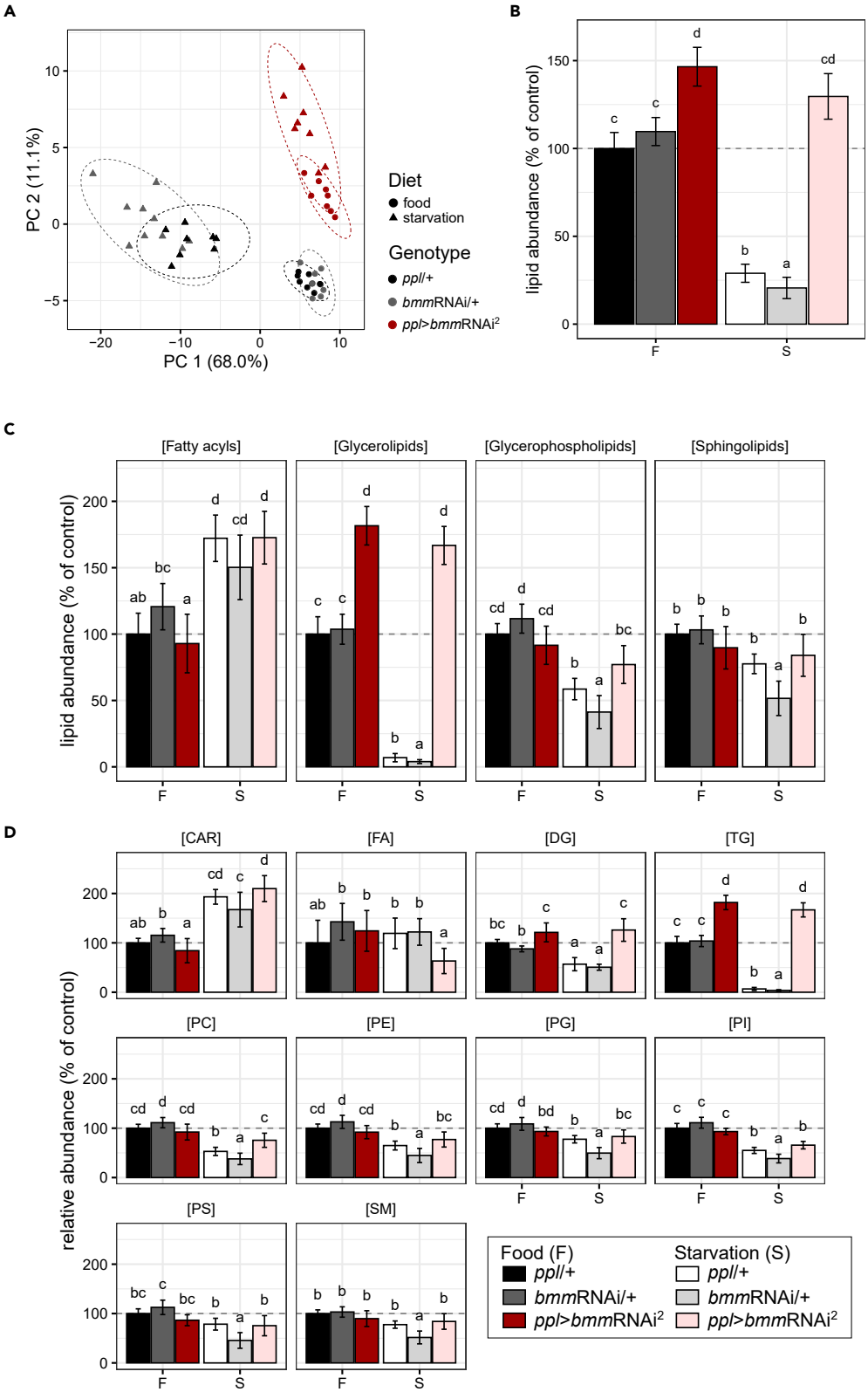
A
PC 2 (11.1%)
PC 1 (68.0%)
Diet
food
starvation
Genotype
ppl/+
bmmRNAi/+
ppl>bmmRNAi2
B
lipid abundance (% of control)
F
S
C
[Fatty acyls]
[Glycerolipids]
[Glycerophospholipids]
[Sphingolipids]
lipid abundance (% of control)
D
[CAR]
[FA]
[DG]
[TG]
[PC]
[PE]
[PG]
[PI]
[PS]
[SM]
relative abundance (% of control)
Food (F)
ppl/+
bmmRNAi/+
ppl>bmmRNAi2
Starvation (S)
ppl/+
bmmRNAi/+
ppl>bmmRNAi2

Figure 4. fb*bmm*KD flies maintain high levels of glycerolipids and phosphatidylcholines under starvation

Analysis of control (*ppl*/+ and *bmm*RNAi/+) and fb*bmm*KD (*ppl* > *bmm*RNAi^{2}) flies under fed (F) and starved (72 h) (S) conditions. Lipid samples from whole flies were analyzed by LC-MS.

(A) Principal component analysis, dashed ellipses indicate 95% confidence interval.

(B) Overall lipid abundance as percent of lipid concentration in fed control (*ppl*/+) flies.

(C) Abundance of distinct lipid groups: fatty acyls, glycerolipids, glycerophospholipids, and sphingolipids as percent of lipid concentration in fed control (*ppl*/+) flies.

(D) Abundance of distinct lipid classes: CAR, acylcarnitines; FA, fatty acids; DG, diacylglycerol; TG, triacylglycerol; PC, phosphatidylcholine; PE, phosphatidylethanolamine; PG, phosphatidylglycerol; PI, phosphatidylinositol; PS, phosphatidylserine; SM, sphingomyelin, as percent of lipid concentration in fed control (*ppl*/+) flies. (B-D) Tukey post hoc test was used to determine significant differences between groups. Different letters were used to indicate significant ($p < 0.05$) differences between groups.

flies (Figure 4A). Overall lipid abundance was significantly decreased in starved control flies (Figure 4B). In contrast, starved fb*bmm*KD flies maintained their whole-body lipid abundance on the pre-starved, fed level (Figure 4B). A closer look at distinct lipid groups revealed that the strongest regulation was present in the group of glycerolipids (Figure 4C). Here, fed and starved fb*bmm*KD flies had dramatically higher levels than both groups of control flies, whereas in other lipid groups significant regulation was only detectable in comparison with either driver or RNAi control flies (Figure 4C). Next, a detailed lipid class analysis showed that the observed glycerolipid increase in fb*bmm*KD flies was mainly caused by the maintenance of high diacylglycerol (DAG) and TAG levels under starvation (Figure 4D). In addition, phosphatidylcholine levels were preserved on the fed level in fb*bmm*KD flies (Figure 4D).

These data show that perturbation of fat body lipolysis in *Drosophila* results in the preservation of lipid stores, a process that is likely to lead to improved compensation for the energy deficit caused by starvation.

fb*bmm*KD flies preserve high levels of saturated short fatty acyl chains under starvation

In contrast to the TAG increase in starved fb*bmm*KD flies, higher DAG levels remained unexplained. Perturbation of TAG hydrolysis should actually result in higher TAG levels and reduced DAGs, as previously described by Ahmadian and colleagues in adipose tissue-specific ATGL-deficient mice (Ahmadian et al., 2011). Thus, the question arose whether in addition to defective lipolysis the lack of *bmm* regulates other lipid metabolic pathways. High DAG levels in starved fb*bmm*KD flies could also be the result of a stimulated new synthesis or *de novo* lipogenesis. It has recently been shown that a lipogenic phenotype is characterized by the increased occurrence of short fatty acyl chains with increased lipid saturation (Lee et al., 2020; Rysman et al., 2010). Detailed analysis of fatty acyl chain length and their degree of saturation revealed that, in contrast to control flies, fb*bmm*KD flies maintain high levels of saturated short-chain fatty acids under starvation (Figure 5A). Further analysis of key lipogenic genes in *Drosophila* such as *dLipin*, a phosphatidate phosphatase converting phosphatidate to DAG (Donkor et al., 2007; Ugrankar et al., 2011), *dTorsin*, a repressor of *dLipin* (Heier and Kuhnlein, 2018), *Acetyl-CoA-Carboxylase (ACC)*, and *Midway (mdy)*, a DAG acyltransferase converting DAG to TAG (Buszczak et al., 2002; Heier and Kuhnlein, 2018), showed that some of these genes are differentially regulated in control and fb*bmm*KD flies, among which *mdy* was most strikingly up-regulated in starved fb*bmm*KD flies (Figure 5B). Finally, fat body-specific knockdown of mdy in fb*bmm*KD flies reversed the protective cardiac phenotype of fb*bmm*KD flies under starvation (Figure 5C).

In summary, these results suggest that the observed higher lipid abundance in starved fb*bmm*KD flies may not only result from defective lipolysis but also may involve the stimulation of lipogenesis under starvation.

DISCUSSION

The role of adipose tissue lipolysis as an energy-providing process for other organs of high-energy demand, such as the heart, is only incompletely understood. This may become particularly important during situations of energy deprivation. Here, we show in *Drosophila melanogaster* that blockade of fat body lipolysis during starvation maintains local lipid stores, likely resulting from the regulation of lipolytic and potentially lipogenic pathways. Together, these processes mediate higher systemic energy substrate levels,

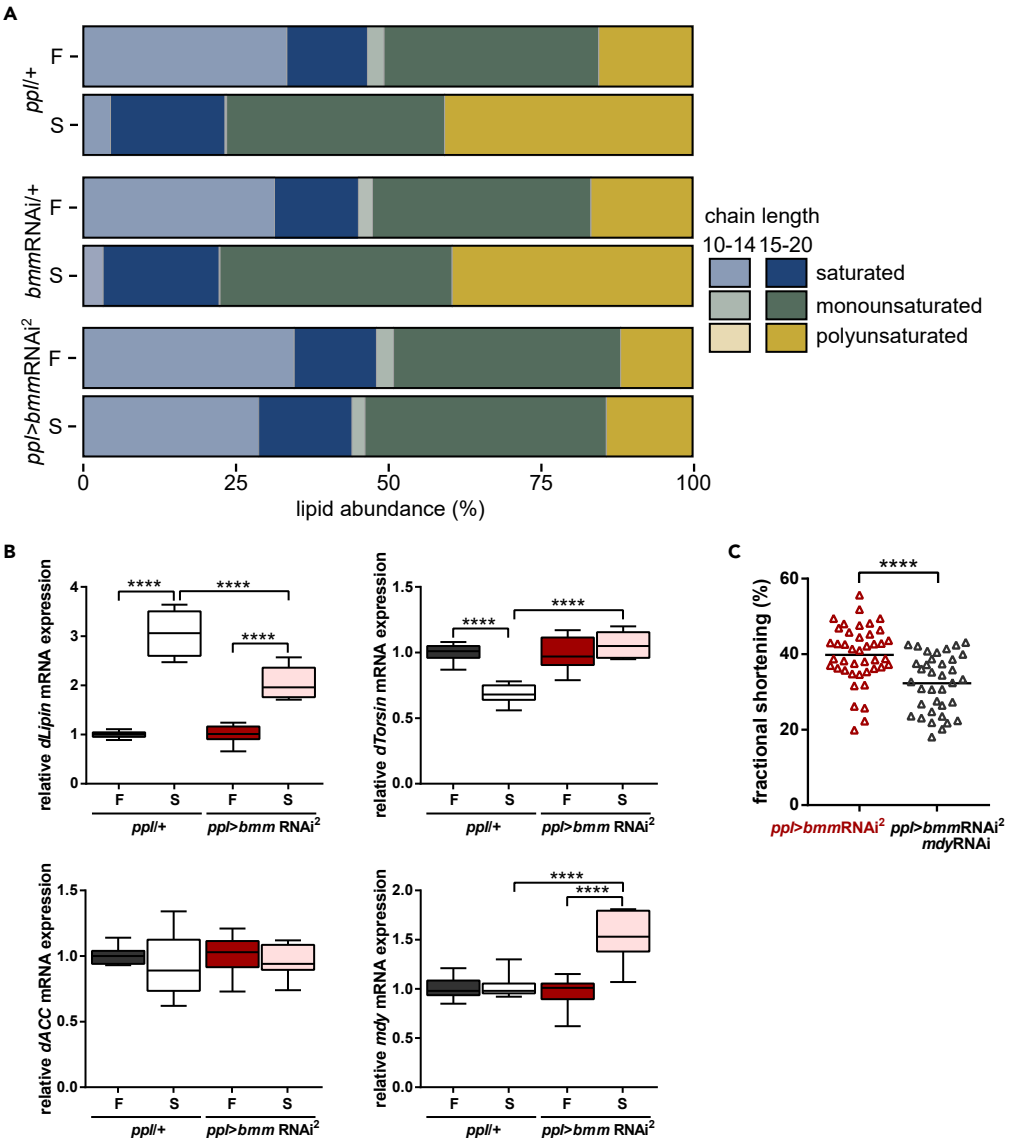

Figure 5. fbbmmKD flies preserve high levels of saturated short fatty acyl chains under starvation

(A) Relative abundance of fatty acyl chain length and average degree of saturation as median composition (%) by sample group (see methods for further details).

(B) Relative mRNA expression in whole flies under fed (F) and starved (72 h) (S) conditions. *dACC*, acetyl-CoA carboxylase; *mdy*, midway. Two-way ANOVA, Bonferroni post hoc test, ****$p < 0.0001$.

(C) Fractional shortening from SOHA analysis of fb*bmm*KD (*ppl* > *bmm*RNAi^2) and *ppl* > *bmm*RNAi^2;mdy RNAi flies under starved conditions. (N = 3, n = 36–42, mean, unpaired t test, ****$p < 0.0001$).

which protected the fly heart against starvation-induced ATP deprivation accompanied by an improvement of contractile function and life-prolonging effects during starvation.

First, we investigated the cardiac phenotype of fb*bmm*KD flies under basal conditions. No major differences were detected between control and fb*bmm*KD flies. This is in contrast to the previously observed contractile deficits in *bmm* heterozygotes (Diop et al., 2015). The systemic and/or cardiac loss of *bmm/ATGL*-mediated lipolysis as observed in *bmm* heterozygotes seems to be deleterious for heart function and must be distinguished from the specific loss in adipose tissue/fat body. This is in line with data from mice showing that systemic loss of *ATGL* results in severe cardiac dysfunction and premature death

(Haemmerle et al., 2006). On the contrary, adipose tissue-specific deletion of *ATGL* protects the heart against pressure-induced heart failure (Kintscher et al., 2020; Salatzki et al., 2018).

Under food deprivation control flies exhibited a reduced lifespan and clear contractile deficits in the heart, a phenomenon previously described in rodents after prolonged starvation (Lee et al., 2015). Perturbation of fat body lipolysis during starvation in fb*bmm*KD flies resulted in a significant lifespan extension and maintenance of regular cardiac function. Starvation resistance with lifespan extension has been previously described in *bmm* mutant flies by Grönke and colleagues (2005). *Bmm* mutants exhibited increased storage fat and markedly outlived control flies under food-deprived conditions (Gronke et al., 2005). Our data now demonstrate that this previously observed improved starvation resistance with lifespan extension is mediated by the reduction of *bmm*-mediated lipolysis specifically in the fat body. Since adult starvation resistance in *Drosophila* mainly depends on total stored calories (Djawdan et al., 1998; Kezos et al., 2017), this study may suggest that reduced fat body lipolysis and subsequent decelerated TAG mobilization results in a gain of caloric storage, sustained energy fueling, maintenance of cardiac function and prolonged survival under starvation (Gronke et al., 2005).

Maintenance of normal cardiac function under starvation in fb*bmm*KD flies was associated with a distinct metabolomic and lipidomic profile compared with control flies. Profiles in control flies appear to correspond to a state of advanced starvation (McCue, 2010). The fb*bmm*KD flies, on the other hand, seem to be protected from fast consumption of energy substrates and exhibit a metabolite/lipid pattern recently described for earlier stages of starvation (Holecek et al., 2001). A closer look at the metabolite profile showed significantly increased levels of BCAAs and lipid intermediates in fb*bmm*KD flies. However, genetically increased BCAAs in *bcat* mutant flies or exogenous re-supply of BCAAs were not able to rescue contractile function in control flies, in contrast to a partial rescue by re-supply of FAs. Further MS-based lipidomics revealed the maintenance of high glycerolipid levels in fb*bmm*KD flies making it likely that lipid energy substrates compensate for the starvation-induced energy deficit and maintain cardiac contractile function.

The question now arises how lipid energy substrates for the rescue of the starved myocardium can be provided at all in the absence of TAG hydrolysis. One explanation would be that *bmm* knockdown in fat body leads to deceleration of lipolysis but TAG hydrolysis still occurs at low level providing energy substrates for cardiac energy production. This maintenance of lipolysis in fb*bmm*KD flies could be mediated by alternative fat body lipases including hormone-sensitive lipase (*dHSL*) or doppelganger von brummer (*dob*) (Gronke et al., 2005; Heier and Kuhnlein, 2018). Another explanation could be the regulation of other lipid metabolic pathways in fb*bmm*KD flies. Previous reports documented that adipose tissue lipolysis is tightly coupled to lipogenesis (Mottillo et al., 2014; Schreiber et al., 2015). In contrast to our data, in these studies pharmacological induction of adipose tissue lipolysis in mice fed a normal chow diet induced lipogenesis and absence of adipose tissue lipolysis decreased lipogenesis under high-fat diet feeding (Mottillo et al., 2014; Schreiber et al., 2015). In our study, a lipogenic lipid and gene expression profile was induced in fb*bmm*KD flies under starvation. These data are consistent with a previously observed up-regulation of the fatty acid synthase gene expression in *bmm* mutant flies (Diop et al., 2015). It appears that, under conditions of energy depletion, perturbation of lipolysis may be able to induce lipogenesis to rescue systemic energy supply, whereas under conditions of energy excess the shutdown of lipolysis also stops lipogenesis. At first glance, the simultaneous occurrence of lipogenesis and energy production via fatty acid oxidation seems paradoxical. However, previous studies described the simultaneous induction of both processes in skeletal muscle, memory T cells, and in brown adipose tissue (O'Sullivan et al., 2014; Solinas et al., 2004; Yu et al., 2002). One could therefore speculate that the improved cardiac energy supply during starvation in fb*bmm*KD flies is mediated by decelerated lipolysis and simultaneously elevated lipogenesis, which together result in the continued supply of lipid-based energy substrates.

Finally, our data point toward *mdy* as a potential target gene under lipolytic regulation. *Mdy* encodes an acyl coenzyme A, structurally related to mammalian DAG-acyltransferase-1 (*DGAT-1*), with a crucial function in TAG formation (Buszczak et al., 2002; Heier and Kuhnlein, 2018). We show that *mdy* is involved in the protective cardiac phenotype of fb*bmm*KD flies. Whether other lipogenic genes are involved in these processes, and how the lack of *bmm* mediates *mdy* up-regulation, requires further investigations.

Energy depletion not only occurs in situations of exogenous shortage of food resources (McCue, 2010) but also plays a crucial role in the clinical setting of catabolic stress during cachexia (Petruzzelli and Wagner, 2016). Of more importance, it is now well established that cancer-mediated cachexia is closely accompanied by cardiac dysfunction and heart failure (Springer et al., 2014). Here, we show in *Drosophila melanogaster* that blockade

of fat body lipolysis during starvation maintains local energy stores and higher systemic energy substrate levels. This protects the fly heart against starvation-induced ATP deprivation associated with an improvement of contractile function and life-prolonging effects during starvation. These results may be also used to expand future studies toward protective new approaches in cachexia-associated cardiac dysfunction.

Limitations of the study

Our study has distinct limitations. Inhibition of lipolysis fb*bmm*KD flies likely results in multiple metabolic changes during starvation. Our data only provides an indirect link between the metabolic profile of fb*bmm*KD flies and the cardiac phenotype. Further mechanistic proof, e.g., that lipogenesis is involved, would require additional experiments. Second, metabolomics and lipidomic analyses were performed in whole flies and not on the tissue level. Third, by focusing on *bmm* we did not clarify whether other interventions that increase lipid stores in flies would result in similar phenotypes.

Resource availability

Lead contact

Further information and requests for resources and reagents should be directed to and will be fulfilled by the lead contact, Dr. Anna Foryst-Ludwig (anna.foryst@charite.de).

Materials availability

Available through lead contact.

Data and code availability

Metabolomics and lipidomics data are available at Mendeley data: https://dx.doi.org/10.17632/jpnds6gr9d.1.

METHODS

All methods can be found in the accompanying transparent methods supplemental file.

SUPPLEMENTAL INFORMATION

Supplemental information can be found online at https://doi.org/10.1016/j.isci.2021.102288.

ACKNOWLEDGMENTS

This study was supported by the BMBF (German Ministry of Education and Research): BfR1328-564 and German Centre for Cardiovascular Research (DZHK) BER 5.4 PR. A.B. is supported by the DZHK;BER 5.4 PR. U.K. is supported by the DZHK; BER 5.4 PR, the Deutsche Forschungsgemeinschaft (DFG – KI 712/10-1), the BMBF/BfR1328-564 and the Einstein Foundation/ Foundation Charité (EVF-BIH-2018-440). R.B. is supported by grants R01 HL54732 and P01 AG033456 from NIH. We thank scivisto for the support with the graphical abstract.

AUTHOR CONTRIBUTIONS

A.B. substantially contributed to conception and design of the study, acquisition of data, and data analysis and interpretation; drafted the article; and revised the article critically for important intellectual content. G.V. contributed substantially to conception and design of the study and data analysis and interpretation. S.D. substantially contributed to conception and design of the study, acquisition of data, and data analysis and interpretation and revised the article critically for important intellectual content. S.B.D. substantially contributed to conception and design of the study and data analysis and interpretation and revised the article critically. C.J. substantially contributed to conception of the study, acquisition of data, and data analysis and interpretation (MS analysis). J.G., S.L., E.K.W., B.H., K.R. contributed to conception of the study, acquisition of data, and data analysis and interpretation (J.G., S.L., B.H.: Drosophila, SOHA; E.K.W., K.R.: Seahorse). A.F.L., J.S., S.S. substantially contributed to conception and design of the study and data analysis and interpretation and revised the article critically for important intellectual content. R.B. and U.K. substantially contributed to conception and design of the study and data analysis and interpretation, drafted the article, and revised the article critically for important intellectual content, and substantially contributed to acquisition of funding. All authors finally approved the version to be published.

DECLARATION OF INTERESTS

The authors declare no competing interests.

Received: August 25, 2020
Revised: February 8, 2021
Accepted: March 4, 2021
Published: April 23, 2021

REFERENCES

Ahmadian, M., Abbott, M.J., Tang, T., Hudak, C.S., Kim, Y., Bruss, M., Hellerstein, M.K., Lee, H.Y., Samuel, V.T., Shulman, G.I., et al. (2011). Desnutrin/ATGL is regulated by AMPK and is required for a brown adipose phenotype. Cell Metab. *13*, 739–748.

Bertero, E., and Maack, C. (2018). Metabolic remodelling in heart failure. Nat. Rev. Cardiol. *15*, 457–470.

Buszczak, M., Lu, X., Segraves, W.A., Chang, T.Y., and Cooley, L. (2002). Mutations in the midway gene disrupt a Drosophila acyl coenzyme A: diacylglycerol acyltransferase. Genetics *160*, 1511–1518.

Diop, S.B., Bisharat-Kernizan, J., Birse, R.T., Oldham, S., Ocorr, K., and Bodmer, R. (2015). PGC-1/Spargel counteracts high-fat-diet-induced obesity and cardiac lipotoxicity downstream of TOR and brummer ATGL lipase. Cell Rep. *10*, 1572–1584.

Djawdan, M., Chippindale, A.K., Rose, M.R., and Bradley, T.J. (1998). Metabolic reserves and evolved stress resistance in *Drosophila melanogaster*. Physiol. Zool. *71*, 584–594.

Donkor, J., Sariahmetoglu, M., Dewald, J., Brindley, D.N., and Reue, K. (2007). Three mammalian lipins act as phosphatidate phosphatases with distinct tissue expression patterns. J. Biol. Chem. *282*, 3450–3457.

Dube, J.J., Sitnick, M.T., Schoiswohl, G., Wills, R.C., Basantani, M.K., Cai, L., Pulinilkunnil, T., and Kershaw, E.E. (2015). Adipose triglyceride lipase deletion from adipocytes, but not skeletal myocytes, impairs acute exercise performance in mice. Am. J. Physiol. Endocrinol. Metab. *308*, E879–E890.

Gronke, S., Mildner, A., Fellert, S., Tennagels, N., Petry, S., Muller, G., Jackle, H., and Kuhnlein, R.P. (2005). Brummer lipase is an evolutionary conserved fat storage regulator in Drosophila. Cell Metab. *1*, 323–330.

Haemmerle, G., Lass, A., Zimmermann, R., Gorkiewicz, G., Meyer, C., Rozman, J., Heldmaier, G., Maier, R., Theussl, C., Eder, S., et al. (2006). Defective lipolysis and altered energy metabolism in mice lacking adipose triglyceride lipase. Science *312*, 734–737.

Heier, C., and Kuhnlein, R.P. (2018). Triacylglycerol metabolism in *Drosophila melanogaster*. Genetics *210*, 1163–1184.

Holecek, M., Sprongl, L., and Tilser, I. (2001). Metabolism of branched-chain amino acids in starved rats: the role of hepatic tissue. Physiol. Res. *50*, 25–33.

Kezos, J.N., Cabral, L.G., Wong, B.D., Khou, B.K., Oh, A., Harb, J.F., Chiem, D., Bradley, T.J., Mueller, L.D., and Rose, M.R. (2017). Starvation but not locomotion enhances heart robustness in Drosophila. J. Insect Physiol. *99*, 8–14.

Kintscher, U., Foryst-Ludwig, A., Haemmerle, G., and Zechner, R. (2020). The role of adipose triglyceride lipase and cytosolic lipolysis in cardiac function and heart failure. Cell Rep. Med. *1*, 100001.

Lee, S.R., Ko, T.H., Kim, H.K., Marquez, J., Ko, K.S., Rhee, B.D., and Han, J. (2015). Influence of starvation on heart contractility and corticosterone level in rats. Pflugers Arch. *467*, 2351–2360.

Lee, Y., Lai, H.T.M., de Oliveira Otto, M.C., Lemaitre, R.N., McKnight, B., King, I.B., Song, X., Huggins, G.S., Vest, A.R., Siscovick, D.S., et al. (2020). Serial biomarkers of de novo lipogenesis fatty acids and incident heart failure in older adults: the cardiovascular health study. J. Am. Heart Assoc. *9*, e014119.

McCue, M.D. (2010). Starvation physiology: reviewing the different strategies animals use to survive a common challenge. Comp. Biochem. Physiol. A Mol. Integr. Physiol. *156*, 1–18.

Mottillo, E.P., Balasubramanian, P., Lee, Y.H., Weng, C., Kershaw, E.E., and Granneman, J.G. (2014). Coupling of lipolysis and de novo lipogenesis in brown, beige, and white adipose tissues during chronic beta3-adrenergic receptor activation. J. Lipid Res. *55*, 2276–2286.

Neinast, M., Murashige, D., and Arany, Z. (2019). Branched chain amino acids. Annu. Rev. Physiol. *81*, 139–164.

O'Sullivan, D., van der Windt, G.J., Huang, S.C., Curtis, J.D., Chang, C.H., Buck, M.D., Qiu, J., Smith, A.M., Lam, W.Y., DiPlato, L.M., et al. (2014). Memory CD8(+) T cells use cell-intrinsic lipolysis to support the metabolic programming necessary for development. Immunity *41*, 75–88.

Petruzzelli, M., and Wagner, E.F. (2016). Mechanisms of metabolic dysfunction in cancer-associated cachexia. Genes Dev. *30*, 489–501.

Rysman, E., Brusselmans, K., Scheys, K., Timmermans, L., Derua, R., Munck, S., Van Veldhoven, P.P., Waltregny, D., Daniels, V.W., Machiels, J., et al. (2010). De novo lipogenesis protects cancer cells from free radicals and chemotherapeutics by promoting membrane lipid saturation. Cancer Res. *70*, 8117–8126.

Salatzki, J., Foryst-Ludwig, A., Bentele, K., Blumrich, A., Smeir, E., Ban, Z., Brix, S., Grune, J., Beyhoff, N., Klopfleisch, R., et al. (2018). Adipose tissue ATGL modifies the cardiac lipidome in pressure-overload-induced left ventricular failure. PLoS Genet. *14*, e1007171.

Schreiber, R., Hofer, P., Taschler, U., Voshol, P.J., Rechberger, G.N., Kotzbeck, P., Jaeger, D., Preiss-Landl, K., Lord, C.C., Brown, J.M., et al. (2015). Hypophagia and metabolic adaptations in mice with defective ATGL-mediated lipolysis cause resistance to HFD-induced obesity. Proc. Natl. Acad. Sci. U S A *112*, 13850–13855.

Shibata, R., Sato, K., Pimentel, D.R., Takemura, Y., Kihara, S., Ohashi, K., Funahashi, T., Ouchi, N., and Walsh, K. (2005). Adiponectin protects against myocardial ischemia-reperfusion injury through AMPK- and COX-2-dependent mechanisms. Nat. Med. *11*, 1096–1103.

Solinas, G., Summermatter, S., Mainieri, D., Gubler, M., Pirola, L., Wymann, M.P., Rusconi, S., Montani, J.P., Seydoux, J., and Dulloo, A.G. (2004). The direct effect of leptin on skeletal muscle thermogenesis is mediated by substrate cycling between de novo lipogenesis and lipid oxidation. FEBS Lett. *577*, 539–544.

Springer, J., Tschirner, A., Haghikia, A., von Haehling, S., Lal, H., Grzesiak, A., Kaschina, E., Palus, S., Potsch, M., von Websky, K., et al. (2014). Prevention of liver cancer cachexia-induced cardiac wasting and heart failure. Eur. Heart J. *35*, 932–941.

Sweeney, G. (2010). Cardiovascular effects of leptin. Nat. Rev. Cardiol. *7*, 22–29.

Ugrankar, R., Liu, Y., Provaznik, J., Schmitt, S., and Lehmann, M. (2011). Lipin is a central regulator of adipose tissue development and function in Drosophila melanogaster. Mol. Cell. Biol. *31*, 1646–1656.

Yu, X.X., Lewin, D.A., Forrest, W., and Adams, S.H. (2002). Cold elicits the simultaneous induction of fatty acid synthesis and beta-oxidation in murine brown adipose tissue: prediction from differential gene expression and confirmation in vivo. FASEB J. *16*, 155–168.

Zechner, R. (2015). Fat FLUX: enzymes, regulators, and pathophysiology of intracellular lipolysis. EMBO Mol. Med. *7*, 359–362.

iScience, Volume *24*

Supplemental information

Fat-body brummer lipase determines survival and cardiac function during starvation in *Drosophila melanogaster*

Annelie Blumrich, Georg Vogler, Sandra Dresen, Soda Balla Diop, Carsten Jaeger, Sarah Leberer, Jana Grune, Eva K. Wirth, Beata Hoeft, Kostja Renko, Anna Foryst-Ludwig, Joachim Spranger, Stephan Sigrist, Rolf Bodmer, and Ulrich Kintscher

Supplemental Information

Figure S1. Basal cardiac phenotype in two-week-old fb*bmm*KD flies. Related to Figure 1

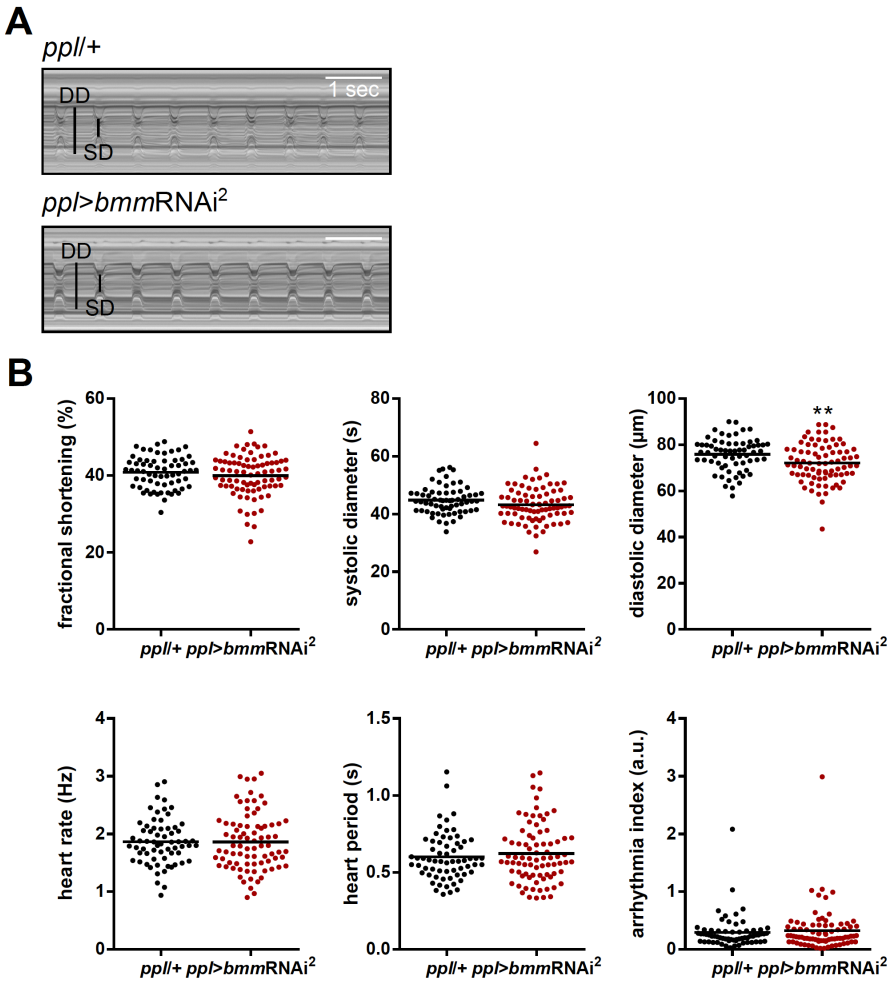

(A) Representative M-modes from SOHA recordings. DD: diastolic diameter, SD: systolic diameter. **(B)** Heart function parameters determined using SOHA. (N = 4, n = 65/81, mean). Unpaired t-test, ** $p < 0.01$, arrhythmia index: Mann-Whitney test.

Figure S2. Cardiac phenotypes of *bcat* mutant flies and BCAA/ FA-mix supplementation. Related to Figure 3.

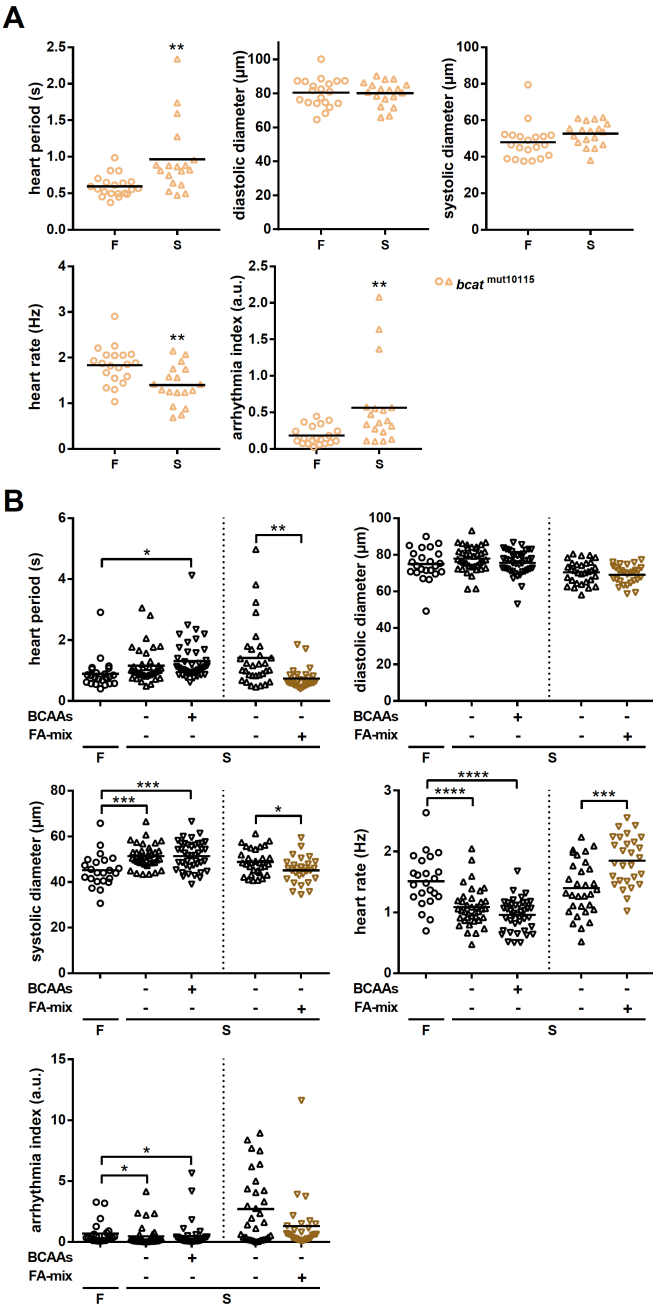

(A) Heart function parameters determined using SOHA of fed (F) and starved (37-41 h) (S) *bcat* mutant flies (BDSC # 10115). (N = 2, F: n = 20, S: n = 18, mean). bcat = branched-chain amino acid transaminase. Unpaired t-test, ** $p < 0.01$, arrhythmia index: Mann-Whitney test, ** $p < 0.01$. **(B)** Heart function parameters determined using SOHA of fed (F) and starved (72 h) (S) *ppl*/+ flies. During starvation, flies received branched chain amino acid (BCAA) supplementation (BCAAs +: 10 mM Ile, 10 mM Leu, 10 mM Val) or H_2O (BCAAs -) as control. BCAA supplemented group also received BCAA mix during heart function analysis. (F: N = 3, n = 23, S: N = 3, n = 38/41, mean) Furthermore, heart function parameters from SOHA analysis of starved *ppl*/+ flies receiving lipid-rich BSA in saline (FA-mix) were determined. (N = 3, n = 46/44, mean). One-way ANOVA, Bonferroni post-hoc test, * $p < 0.05$, *** $p < 0.001$, **** $p < 0.0001$, arrhythmia index: Kruskal-Wallis test, Dunn's post-hoc test, * $p < 0.05$ (BCAA). Unpaired t-test, *** $p < 0.001$, arrhythmia index: Mann-Whitney test, * $p < 0.05$, ** $p < 0.01$, *** $p < 0.001$ (FA-mix).

Supplemental Table S1. List of Drosophila strains used in this study. Related to Figure 1 - 5.

Experimental Models: Organisms/Strains		
Drosophila melanogaster: UAS-*bmm* RNAi (II)	Vienna *Drosophila* Resource Center (VDRC)	VDRC 37877
Drosophila melanogaster: UAS-*bmm* RNAi (III)	VDRC	VDRC 37880
Drosophila melanogaster: GD control	VDRC	VDRC 60000
Drosophila melanogaster: ppl-Gal4	Bloomington *Drosophila* Stock Center (BDSC)	BDSC 58768
Drosophila melanogaster: w^{1118}	BDSC	BDSC 5905
Drosophila melanogaster: UAS- *bmm* RNAi (II); UAS-*bmm* RNAi (III)	This paper.	N/A
Drosophila melanogaster: *ppl>bmm*RNAi^{2}	This paper.	N/A
Drosophila melanogaster: *bcat* ^{mut10115}	BDSC	BDSC 10115
Drosophila melanogaster: UAS-*mdy* RNAi (III)	VDRC	VDRC 6367

Transparent Methods

Contact for Reagent and Resource Sharing

Dr. Anna Foryst-Ludwig: anna.foryst@charite.de

Deposited Data

Mendeley data: http://dx.doi.org/10.17632/jpnds6gr9d.1

Experimental Model and Subject Details

Drosophila melanogaster were kept at room temperature in a 12 h light-dark cycle receiving standardized food (Formula 4-24®). For experiments, two-week-old males were used.

Method Details

- **Starvation experiments**

For starvation experiments, two-week-old male flies were kept in starvation vials containing 1% agar at 18°C for 3 days. To determine starvation resistance, 10 starvation vials with 10 flies each were monitored. Survival was visually examined every three hours during daytime until all flies were dead.

- **Semi-automated optical heart beat analysis**

Analysis of cardiac function was performed according to Fink et al., Ocorr et al. and Vogler et al. (Fink et al., 2009; Ocorr et al., 2009; Vogler and Ocorr, 2009). For the semi-intact *Drosophila* heart tube dissection, flies were anesthetized using FlyNap® (Carolina Biological Supply Company) and heart tube was carefully exposed by removal of head, ventral nerve cord, ventral abdominal cuticle and internal organs. During the dissection, flies were bathed in oxygenated artificial hemolymph or saline (artificial hemolymph without carbohydrates) according to Fink (Fink et al., 2009). Moreover, heart tube was cleared from surrounding fat

body at abdominal segment 2 and 3 using suction from fine glass micropipettes. Heart tubes were allowed to equilibrate for 20 min until recording.

Using an upright light microscope (DM6B, Leica), a 10x water immersion lens (W N-Achroplan 10x/0,3 M27, Leica), and a digital CMOS camera (ORCA-Flash 4.0 V2 camera, Hamamatsu) beating heart tubes were recorded at the 3rd abdominal segment. HCImage Acquisition software (Hamamatsu) was used to record the movies, with exposure time set to 7 ms, frame rate of 128 fps and 30 s total movie length. Movies of beating heart tubes were analyzed using the semi-automated optical heartbeat analysis (SOHA) software.

For oligomycin experiment, prepared hearts equilibrated for 15 min and were then incubated with artificial hemolymph containing 2.5 µM oligomycin (Sigma-Aldrich) or dimethyl sulfoxide (Sigma-Aldrich) as vehicle for 10 min. Afterwards, heartbeats were recorded as described.

For rescue experiments, BCAAs (10 mM isoleucine, 10 mM leucine, 10 mM valine) or lipid-rich BSA (1 mg/ml; AlbuMAX II, ThermoFisher) were added to saline and heart function measured as described.

- **TAG measurement**

Based on a protocol published by Diop et al. (Diop et al., 2017) whole-body triacylglycerol (TAG) levels were measured. Briefly, flies were weighed for normalization and frozen at -20°C. Three flies were pooled for one sample and homogenized in PBST (PBS + 0.05 % Triton X-100) using ceramic beads and the SpeedMill Plus system (Analytik Jena). After centrifugation, TAG levels were determined in the supernatant using the Triglyceride FS kit (DiaSys) and normalized to fly weight.

- **Gene expression analysis**

For gene expression analyses mRNA was isolated from whole flies (10 flies/sample) or abdomen (8-11 abdomen/sample). Whole flies or abdomen were frozen and homogenized in 300 µl QIAzol lysis reagent (Qiagen) using a pellet pestle cordless motor (Kimble). After

centrifugation, chloroform was added for nucleic acid extraction. Next, isopropanol was added for RNA precipitation, samples incubated at 31°C for 10 min and subsequently centrifuged. Finally, RNA pellet was washed multiple times with 75% ethanol, dried and dissolved in RNAse-free H_2O. cDNA was synthesized from RNA using reverse transcriptase, RNAsin and dNTPs (Promega) according to manufacturers' protocol. Using quantitative RT-PCR, gene expression was analyzed. For this, SYBR Green (Applied Biosystems) was added as DNA-intercalating fluorescent dye. Expression levels of two reference genes, namely *Drosophila* actin (*act5c*) and ribosomal protein L32 (*RpL32*), were used to normalize the data using the $2^{-\Delta\Delta ct}$ method (Livak and Schmittgen, 2001).

- **Immunohistochemistry**

Heart tubes were carefully exposed in oxygenated artificial hemolymph and all remaining fat was removed (Alayari et al., 2009; Vogler and Ocorr, 2009). Artificial hemolymph was replaced with relaxing buffer (5 mM EGTA in artificial hemolymph) and hearts fixed with 4% paraformaldehyde for 20 min. After several washing steps with PBSTx (PBS + 0.3% Triton-X 100), hearts were blocked with 10% normal goat serum at room temperature for 1 hr. Next, heart tubes were incubated with Alexa Fluor 488 Phalloidin (1:500, Thermo Fisher Scientific) to stain F-actin at 4°C overnight with continual shaking. Afterwards, hearts were washed again with PBS and finally mounted using Dako mounting medium (Agilent). Hearts were imaged using a 63x oil immersion objective on a Leica SPE confocal microscope.

- **Polar metabolite profiling**

For metabolomics analysis, flies were flash-frozen in liquid nitrogen and homogenized in groups of three in 300 µl ice-cold 75% methanol using a pellet pestle motor (Kimble). Next, 750 µl methyl tert-butyl ether (Biosolve) was added, samples shaken for 10 min at room temperature and 175 µl UPLC-H_2O added. After incubation for 10 min at room temperature,

samples were thoroughly mixed and centrifuged. In this study, polar and semipolar metabolites from the (lower) polar phase were investigated. Finally, 100 µl were taken from the lower phase and dried in a vacuum centrifuge.

Metabolites were separated using gas-chromatography (7890B, Agilent), and ionization of metabolites was achieved using atmospheric-pressure chemical ionization. Mass-to-charge ratio of ionized metabolites was determined with the Impact II quadrupole time-of-flight (QqTOF) mass spectrometer (Bruker) (Jaeger et al., 2016).

Both retention time and mass-to-charge ratio were used for identification of metabolites. For this, the MRMPROBS (Multiple Reaction Monitoring based PROBabilistic System for widely targeted metabolomics) and an in-house compound library of approximately 400 primary metabolites were used. Intensities were normalized to the sum of all detected peak intensities, and data finally corrected for run order effects (Jaeger and Lisec, 2018). In total, 193 metabolites were identified.

- **Lipidomics**

Lipid samples from above were reconstituted and separated by liquid chromatography (Lisec et al., 2019). Each sample was analyzed in positive and negative mode electrospray ionization (ESI+/-) using a DuoSpray ion source (SCIEX) operated at 320 °C and at capillary voltages of 5500 V and 4500 V, respectively. For detection, a TripleTOF mass spectrometer (SCIEX) was used in full-scan mode with an m/z range 100-1200 and a scan rate of 4 s^{-1}. MS/MS spectra were recorded in data-dependent mode (DDA Top-4). For identification and quantification, data was processed with MS-DIAL (Tsugawa et al., 2015), as described (Lisec et al., 2019). A custom R script was used to remove duplicate, ambiguously identified as well as ‘sparse’ lipids, i.e. compounds not detected in 20% or more of the samples of a group. The final lipid list consisted of 399 species. For these, intensities were corrected for run order effects as above. Signals were otherwise kept unnormalized to preserve starving-induced changes to total lipid contents (which were reduced up to five-fold). Principal component analysis was carried out on log-transformed, Pareto-scaled data using the NIPALS algorithm.

Analysis of variance (ANOVA) was similarly calculated on log-transformed data. The Tukey post-hoc test was used to determine significant differences between groups. Different letters were used to indicate significant ($p < 0.05$) differences between groups. For estimation of average chain length and average unsaturation index, the lipid list was narrowed down to those lipids with full MS/MS information, i.e. those spectra that allowed precise determination of lengths and double bond numbers of all fatty acid residues ($n = 296$). Intensities of intact lipids were divided by the number of fatty acid residues (e.g. 2 for phospholipids, 3 for triacylglycerols). These derived intensities were summed by fatty acid species (e.g. 16:0, 16:1) per sample and summarized as median composition (%) by sample group.

- **Oxygen consumption measurements**

To determine oxygen consumption of *Drosophila* hearts, hearts were prepared in saline as described for SOHA, except for the additional removal of entire fat body using careful suction. Moreover, thorax was completely removed, and final abdominal cuticle containing the attached beating heart tube was transferred to a XF96 microplate (Agilent). To assure permanent attachment, vaseline (Fagron) was used to adhere the specimen to the well. After addition of 175 µl DMEM (2 mM glucose, 2 mM L-glutamine, pH 7.4; Sigma-Aldrich) to the well, restraints (Neville et al., 2018) were placed above the specimen to prevent any movement during the measurement. Oxygen consumption measurements were performed using the Seahorse XFe96 Analyzer (Agilent). Mitochondrial respiratory function was assessed using specific inhibitors: 10 µM oligomycin A (Sigma-Aldrich), 5 µM FCCP: Carbonyl Cyanide-p-trifluoromethoxyphenylhydrazone (Sigma-Aldrich), 2.5 µM antimycin A/2.5 µM rotenone (Sigma-Aldrich).

- **Statistical analysis**

Statistical analysis was performed using GraphPad Prism 6, if not otherwise indicated. To compare differences between groups, one- or two-way ANOVA (Bonferroni pots-hoc test), Kruskal Wallis test (Dunn´s post-hoc test), student t-test, or Mann-Whitney test was used, as appropriate (Salatzki et al., 2018). Statistical significance was assumed at $p<0.05$.

Supplemental References

Alayari, N.N., Vogler, G., Taghli-Lamallem, O., Ocorr, K., Bodmer, R., and Cammarato, A. (2009). Fluorescent labeling of Drosophila heart structures. J Vis Exp.

Diop, S.B., Birse, R.T., and Bodmer, R. (2017). High Fat Diet Feeding and High Throughput Triacylglyceride Assay in Drosophila Melanogaster. J Vis Exp.

Fink, M., Callol-Massot, C., Chu, A., Ruiz-Lozano, P., Izpisua Belmonte, J.C., Giles, W., Bodmer, R., and Ocorr, K. (2009). A new method for detection and quantification of heartbeat parameters in Drosophila, zebrafish, and embryonic mouse hearts. Biotechniques *46*, 101-113.

Jaeger, C., Hoffmann, F., Schmitt, C.A., and Lisec, J. (2016). Automated Annotation and Evaluation of In-Source Mass Spectra in GC/Atmospheric Pressure Chemical Ionization-MS-Based Metabolomics. Anal Chem *88*, 9386-9390.

Jaeger, C., and Lisec, J. (2018). Statistical and Multivariate Analysis of MS-Based Plant Metabolomics Data. Methods Mol Biol *1778*, 285-296.

Lisec, J., Jaeger, C., Rashid, R., Munir, R., and Zaidi, N. (2019). Cancer cell lipid class homeostasis is altered under nutrient-deprivation but stable under hypoxia. BMC Cancer *19*, 501.

Livak, K.J., and Schmittgen, T.D. (2001). Analysis of relative gene expression data using real-time quantitative PCR and the 2(-Delta Delta C(T)) Method. Methods *25*, 402-408.

Neville, K.E., Bosse, T.L., Klekos, M., Mills, J.F., Weicksel, S.E., Waters, J.S., and Tipping, M. (2018). A novel ex vivo method for measuring whole brain metabolism in model systems. J Neurosci Methods *296*, 32-43.

Salatzki, J., Foryst-Ludwig, A., Bentele, K., Blumrich, A., Smeir, E., Ban, Z., Brix, S., Grune, J., Beyhoff, N., Klopfleisch, R*., et al.* (2018). Adipose tissue ATGL modifies the cardiac lipidome in pressure-overload-induced left ventricular failure. PLoS Genet *14*, e1007171.

Tsugawa, H., Cajka, T., Kind, T., Ma, Y., Higgins, B., Ikeda, K., Kanazawa, M., VanderGheynst, J., Fiehn, O., and Arita, M. (2015). MS-DIAL: data-independent MS/MS deconvolution for comprehensive metabolome analysis. Nat Methods *12*, 523-526.

Vogler, G., and Ocorr, K. (2009). Visualizing the beating heart in Drosophila. J Vis Exp.